

Analytic Expressions for Fiducial and Surface Target Registration Error

Burton Ma¹ and Randy E. Ellis²

¹ Human Mobility Research Centre, Queen's University, Canada
mab@cs.queensu.ca

² Dept. of Radiology, Brigham & Women's Hospital, USA
ellis@bwh.harvard.edu

Abstract. We propose and test analytic equations for approximating expected fiducial and surface target registration error (TRE). The equations are derived from a spatial stiffness model of registration. The fiducial TRE equation is equivalent to one presented by [1]. We believe that the surface TRE equation is novel, and we provide evidence from computer simulations to support the accuracy of the approximation.

1 Introduction

Many forms of computer-assisted surgery use registration to align patient anatomy to medical imagery. Quantifying registration error and its possible effects on the surgical outcome are of great interest to practitioners of computer-assisted surgery. One task-specific method of measuring registration error is to estimate the target registration error (TRE), which is defined as the error between a measured anatomical target under the registration transformation and its corresponding location in the medical image.

Simulation studies of fiducial TRE have been described in [2,3,4,5] and elsewhere. A statistical derivation of fiducial TRE was described in [1]. Equations predicting surface TRE, where points are measured from a surface and aligned to a model of the surface, have not yet been described, to the best of our knowledge. In this article we show that our spatial stiffness models of fiducial and surface registration yield analytic expressions for TRE that accurately match simulation results.

2 Spatial Stiffness of a Passive Mechanical System

The background material, from the robotics literature, is taken from our previous work [6].

A general model of the elastic behavior of a passive unloaded mechanism is a rigid body that is suspended by linear and torsional springs, which leads to analysis of the spatial stiffness or compliance of the mechanism. For a passive mechanism in local equilibrium, a twist displacement \mathbf{t} of a rigid body is related to a counteracting wrench force \mathbf{w} by a 6×6 spatial stiffness matrix \mathbf{K} :

$$\mathbf{w} = \mathbf{K}\mathbf{t} = \begin{bmatrix} \mathbf{A} & \mathbf{B} \\ \mathbf{B}^T & \mathbf{D} \end{bmatrix} \mathbf{t} \quad (1)$$

where \mathbf{A} , \mathbf{B} , and \mathbf{D} are 3×3 matrices. The twist is a vector $\mathbf{t} = [\mathbf{v}^T \ \boldsymbol{\omega}^T]^T$ where $\mathbf{v}^T = [v_x \ v_y \ v_z]$ is linear displacement and $\boldsymbol{\omega}^T = [\omega_x \ \omega_y \ \omega_z]$ is rotational displacement. The

wrench is a vector $\mathbf{w} = [\mathbf{f}^T \ \boldsymbol{\tau}^T]^T$ where $\mathbf{f}^T = [f_x \ f_y \ f_z]$ is force and $\boldsymbol{\tau}^T = [\tau_x \ \tau_y \ \tau_z]$ is torque. Equation 1 is simply a general, vectorial expression of Hooke’s Law.

\mathbf{K} is a symmetric positive-definite matrix for stable springs and small displacements from equilibrium. The eigenvalues of \mathbf{K} are not immediately useful because their magnitudes change with the coordinate frame used to define \mathbf{K} ; however, it can be shown [7] that the eigenvalues of

$$\mathbf{K}_V = \mathbf{D} - \mathbf{B}^T \mathbf{A}^{-1} \mathbf{B} \quad \text{and} \quad \mathbf{C}_W = \mathbf{A}^{-1} \tag{2}$$

are frame invariant. The eigenvalues μ_1, μ_2, μ_3 of \mathbf{K}_V are the principal rotational stiffnesses, and the eigenvalues $\sigma_1, \sigma_2, \sigma_3$ of \mathbf{C}_W^{-1} are the principal translational stiffnesses.

The screw representation of a twist is a rotation about an axis followed by a translation parallel to the axis. The screw is usually described by the rotation axis, the net rotation magnitude M , with the independent translation specified as a pitch, h , that is the ratio of translational motion to rotational motion. For a twist $h = \boldsymbol{\omega} \cdot \mathbf{v} / \|\boldsymbol{\omega}\|^2$, $M = \|\boldsymbol{\omega}\|$, and the axis of the screw is parallel to $\boldsymbol{\omega}$ passing through the point $\mathbf{q} = \boldsymbol{\omega} \times \mathbf{v} / \|\boldsymbol{\omega}\|^2$. A pure translation (where $\boldsymbol{\omega} = \mathbf{0}$) has $h = \infty$ and $M = \|\mathbf{v}\|$, with the screw axis parallel to \mathbf{v} passing through the origin. A unit twist has magnitude $M = 1$, in which case, for $\boldsymbol{\omega} \neq \mathbf{0}$, $h = \boldsymbol{\omega} \cdot \mathbf{v}$ and $\mathbf{q} = \boldsymbol{\omega} \times \mathbf{v}$. For a small screw motion with $M = \alpha$ and $\boldsymbol{\omega} \neq \mathbf{0}$, a point located at a distance ρ from the screw axis will be displaced by length

$$l \approx |\alpha| \sqrt{\rho^2 + (\boldsymbol{\omega} \cdot \mathbf{v})^2} \tag{3}$$

Equation 3 is the basis of the frame-invariant quality measure for compliant grasps described by [7]. Because the principal rotational and translational stiffnesses have different units, they cannot be directly compared to one another. One solution is to scale the principal rotational stiffnesses by an appropriate factor (see [7] for details) to yield the so-called equivalent stiffnesses, $\mu_{eq,i}$:

$$\mu_{eq,i} = \mu_i / (\rho_i^2 + (\boldsymbol{\omega}_i \cdot \mathbf{v}_i)^2) \quad i = 1, 2, 3 \tag{4}$$

where, μ_i is an eigenvalue of \mathbf{K}_V with an associated eigenvector $\boldsymbol{\omega}_i$, and ρ_i is the distance between the point of interest and the screw axis of the twist $[\mathbf{v}_i^T \ \boldsymbol{\omega}_i^T]^T$.

2.1 Fiducial Registration Stiffness Matrix

We previously described a spatial stiffness model of fiducial registration where each fiducial marker was attached to its noise-free location with a linear spring [8]. The resulting stiffness matrix for fiducial registration with N fiducials centered at the origin was shown to be

$$\mathbf{K} = \begin{bmatrix} N\mathbf{I}_{3 \times 3} & -[\boldsymbol{\Pi} \times] \\ [\boldsymbol{\Pi} \times] & \sum_{i=1}^N \begin{bmatrix} y_i^2 + z_i^2 & -x_i y_i & -x_i z_i \\ -x_i y_i & x_i^2 + z_i^2 & -y_i z_i \\ -x_i z_i & -y_i z_i & x_i^2 + y_i^2 \end{bmatrix} \end{bmatrix} = \begin{bmatrix} \mathbf{A} & \mathbf{B} \\ \mathbf{B}^T & \mathbf{D} \end{bmatrix} \tag{5}$$

where $\mathbf{p}_i = [x_i \ y_i \ z_i]^T$ is the location of the i^{th} fiducial and the matrix $\mathbf{B}^T = [\boldsymbol{\Pi} \times]$ is the cross-product matrix $\begin{bmatrix} 0 & z_i & -y_i \\ -z_i & 0 & x_i \\ y_i & -x_i & 0 \end{bmatrix}$ such that $[\boldsymbol{\Pi} \times] \mathbf{u} = \boldsymbol{\Pi} \times \mathbf{u}$. If the fiducials

are centered at the origin then $\mathbf{B} = \mathbf{B}^T = \mathbf{0}$ which is very unusual for stiffness matrices [8]. Because the principal stiffnesses are invariant under rigid coordinate frame transformation we can assume that the fiducials are centered at the origin without loss of generality. Under this assumption, the principal rotational stiffnesses are the eigenvalues of $\mathbf{K}_V = \mathbf{D} - \mathbf{B}^T \mathbf{A}^{-1} \mathbf{B} = \mathbf{D}$. The matrix \mathbf{D} is the inertia tensor for a system of N point particles of unit mass [9]; thus, the rotational stiffnesses are the principal moments of inertia and the eigenvectors are the principal axes.

2.2 Surface Registration Stiffness Matrix

Our stiffness model for surface registration also used linear springs attached to the registration point, but the other end of the spring was allowed to slide to the nearest corresponding surface point when the registration points were displaced by a small amount [6]. The simplest expression for the stiffness matrix for surface registration with N surface registration points was shown to be

$$\mathbf{K} = \sum_{i=1}^N \begin{bmatrix} \mathbf{n}_i \\ \mathbf{p}_i \times \mathbf{n}_i \end{bmatrix} \begin{bmatrix} \mathbf{n}_i & \mathbf{p}_i \times \mathbf{n}_i \end{bmatrix} = \begin{bmatrix} \mathbf{A} & \mathbf{B} \\ \mathbf{B}^T & \mathbf{D} \end{bmatrix} \quad (6)$$

where \mathbf{p}_i is the i^{th} surface registration point and \mathbf{n}_i is its associated unit normal vector; expanding Equation 6 provides some intuition for optimizing registration point selection [6].

3 Target Registration Error

We hypothesize that TRE can be estimated by considering a constant amount of work done (energy), c , and calculating the displacement of the system. The work done is taken to be the sum $c = c_\delta + c_r$ of two components $c_\delta = c_r$ representing the energies required to respectively translate and rotate the system. The magnitude of the translation and rotation are related to the error in localizing a fiducial marker or surface registration point. We refer to these errors as fiducial localization error (FLE) and point localization error (PLE), and we characterize them by their variances s_{FLE}^2 and s_{PLE}^2 . We explore our hypothesis first for the case of fiducial registration.

3.1 Fiducial Registration TRE

Suppose that the fiducial markers are translated by an amount α_{δ_1} in a direction parallel to \mathbf{v}_1 where \mathbf{v}_1 is the eigenvector associated with the principal translational stiffness σ_1 . Such a translation will induce a TRE of magnitude α_{δ_1} . The work done by this translation is $c_{\delta_1} = \frac{1}{2} \sigma_1 \alpha_{\delta_1}^2$; simple rearrangement yields $\alpha_{\delta_1}^2 = \frac{2c_{\delta_1}}{\sigma_1}$. A similar argument can be used for translations in the directions parallel to \mathbf{v}_2 and \mathbf{v}_3 . The squared translational TRE is $\alpha_\delta^2 = \alpha_{\delta_1}^2 + \alpha_{\delta_2}^2 + \alpha_{\delta_3}^2 = \frac{2c_{\delta_1}}{\sigma_1} + \frac{2c_{\delta_2}}{\sigma_2} + \frac{2c_{\delta_3}}{\sigma_3}$. It seems reasonable to assume that the work done for each direction is equal if the FLE is isotropic; substituting $c_{\delta_1} = c_{\delta_2} = c_{\delta_3} = \frac{c_\delta}{3}$ and $\sigma_1 = \sigma_2 = \sigma_3 = N$ yields

$$\alpha_\delta^2 = \frac{2c_\delta}{N} \quad (7)$$

Suppose the system is rotated about the axis ω_1 where ω_1 is the eigenvector associated with the principal rotational stiffness μ_1 . Such a rotation will induce a TRE; let the magnitude of the TRE be α_{r_1} . The work done by this rotation is $c_{r_1} = \frac{1}{2}\mu_{\text{eq}_1}\alpha_{r_1}^2$; simple rearrangement yields $\alpha_{r_1}^2 = \frac{2c_{r_1}}{\mu_{\text{eq}_1}}$. Using a similar argument for rotations about ω_2 and ω_3 leads to a total squared displacement of $\alpha_r^2 = \alpha_{r_1}^2 + \alpha_{r_2}^2 + \alpha_{r_3}^2 = \frac{2c_{r_1}}{\mu_{\text{eq}_1}} + \frac{2c_{r_2}}{\mu_{\text{eq}_2}} + \frac{2c_{r_3}}{\mu_{\text{eq}_3}}$. Recall that Equation 4 states $\mu_{\text{eq},i} = \mu_i/(\rho_i^2 + (\omega_i \cdot \mathbf{v}_i)^2)$, where μ_i is the principal rotational stiffness, ω_i is the eigenvector associated with μ_i , \mathbf{v}_i is the linear displacement component of the twist vector $\mathbf{t}_i = [\mathbf{v}_i^T \ \omega_i^T]^T$, and ρ_i is the distance between the target and the screw axis of \mathbf{t}_i . It can be shown that \mathbf{v}_i^T and ω_i^T must be mutually perpendicular if $\mathbf{B} = \mathbf{0}$ [10]; therefore $\omega_i \cdot \mathbf{v}_i = 0$ and $\mu_{\text{eq},i} = \mu_i/\rho_i^2$. Assuming the work done is evenly divided among the three rotations and substituting for $\mu_{\text{eq},i}$ gives the squared rotational TRE as

$$\alpha_r^2 = \frac{2c_r\rho_1^2}{3\mu_1} + \frac{2c_r\rho_2^2}{3\mu_2} + \frac{2c_r\rho_3^2}{3\mu_3} \tag{8}$$

Adding the two components are in quadrature and taking the square root yields the root mean squared TRE

$$\text{TRE} = \sqrt{\alpha_\delta^2 + \alpha_r^2} = \sqrt{\frac{2c_\delta}{N} + \frac{2c_r\rho_1^2}{3\mu_1} + \frac{2c_r\rho_2^2}{3\mu_2} + \frac{2c_r\rho_3^2}{3\mu_3}} \tag{9}$$

Amount of Work Done. The amount of work done $c_\delta = c_r$ must be defined to compute an estimate of TRE. It is easiest to compute the work done by translation. Consider the squared displacement of the center of mass α_{com}^2 of a system of N points where the location of each point is subject to zero mean, isotropic noise with variance s^2 . If the centroid of the noise-free points is at the origin the expected value of α_{com}^2 is

$$E[\alpha_{\text{com}}^2] = E[\|\bar{\mathbf{P}}\|^2] = E[\bar{P}_x^2 + \bar{P}_y^2 + \bar{P}_z^2] = E[\bar{P}_x^2] + E[\bar{P}_y^2] + E[\bar{P}_z^2] \tag{10}$$

where $\bar{\mathbf{P}} = [\bar{P}_x \ \bar{P}_y \ \bar{P}_z]^T$ is the mean of the noisy point locations. Two statistical facts are ([11])

$$E[\bar{P}_x] = E[\bar{P}_y] = E[\bar{P}_z] = 0 \tag{11}$$

$$\text{Var}(\bar{P}_x) = \text{Var}(\bar{P}_y) = \text{Var}(\bar{P}_z) = \frac{s^2}{3N} \tag{12}$$

Where Var denotes the variance. Using Equation 11, Equation 10 can be rewritten as

$$\begin{aligned} E[\alpha_\delta^2] &= E[\bar{P}_x^2] + E[\bar{P}_y^2] + E[\bar{P}_z^2] \\ &= E[(\bar{P}_x - E[\bar{P}_x])^2] + E[(\bar{P}_y - E[\bar{P}_y])^2] + E[(\bar{P}_z - E[\bar{P}_z])^2] \end{aligned} \tag{13}$$

For any random variable X the variance of X is defined as $\text{Var}(X) = E[(X - E[X])^2]$. Thus Equation 13 becomes

$$E[\alpha_{\text{com}}^2] = \text{Var}(\bar{P}_x) + \text{Var}(\bar{P}_y) + \text{Var}(\bar{P}_z) = \frac{s^2}{N} \tag{14}$$

To compute the energy associated with the displacement of the center of mass we consider the work done by a single spring with spring constant $k_{\text{com}} = N$ attached to the center of mass. The expected work done is

$$E[c_{\text{com}}] = \frac{1}{2}k_{\text{com}}E[\alpha_{\text{com}}^2] = \frac{1}{2}s^2 \quad (15)$$

Substituting $c_{\text{com}} = c_\delta$ and $s^2 = s_{\text{FLE}}^2$ into Equation 15 gives the expected work done by translation induced by fiducial localization noise as

$$E[c_\delta] = \frac{1}{2}s_{\text{FLE}}^2 \quad (16)$$

Substituting $c_\delta = c_r$ and Equation 16 into Equation 9 gives the TRE for isotropic noise as

$$\text{TRE} = s_{\text{FLE}} \sqrt{\frac{1}{N} + \frac{\rho_1^2}{3\mu_1} + \frac{\rho_2^2}{3\mu_2} + \frac{\rho_3^2}{3\mu_3}} \quad (17)$$

Recall that the μ_i are the principal moments of inertia of the fiducial configuration; squaring Equation 17 yields Equation 46 from [1] for the expected value of TRE^2 .

3.2 Surface Registration TRE

The development of the equations for estimating TRE for surface-based registration is similar to that presented in Section 3.1 for fiducial registration. Rather than repeating large sections of text, we refer the reader to Section 3.1 for details, and present only the relevant equations in this section.

By considering the work done induced by translation along the three principal axes of translation, the squared translational TRE can be written as

$$\alpha_\delta^2 = \frac{2c_\delta}{3} \left(\frac{1}{\sigma_1} + \frac{1}{\sigma_2} + \frac{1}{\sigma_3} \right) \quad (18)$$

By considering the work done by rotation about the three principal axes of rotation, the squared rotational TRE can be written as

$$\alpha_r^2 = \frac{2c_r}{3} \left(\frac{\rho_1^2 + (\boldsymbol{\omega}_1 \cdot \mathbf{v}_1)^2}{\mu_1} + \frac{\rho_2^2 + (\boldsymbol{\omega}_2 \cdot \mathbf{v}_2)^2}{\mu_2} + \frac{\rho_3^2 + (\boldsymbol{\omega}_3 \cdot \mathbf{v}_3)^2}{\mu_3} \right) \quad (19)$$

Addition of Equations 18 and 19 in quadrature yields our estimate for surface registration TRE.

Amount of Work Done. The same argument used for defining the work done in the fiducial registration case (Section 3.1) applies here. The amount of work done by translation is $c_\delta = \frac{1}{2}s_{\text{FLE}}^2$. Equating the energies of translation and rotation, and substituting into Equations 18 and 19 gives the TRE for isotropic noise as

$$\text{TRE} = \frac{s_{\text{FLE}}}{\sqrt{3}} \left[\left(\frac{1}{\sigma_1} + \frac{1}{\sigma_2} + \frac{1}{\sigma_3} \right) + \left(\frac{\rho_1^2 + (\boldsymbol{\omega}_1 \cdot \mathbf{v}_1)^2}{\mu_1} + \frac{\rho_2^2 + (\boldsymbol{\omega}_2 \cdot \mathbf{v}_2)^2}{\mu_2} + \frac{\rho_3^2 + (\boldsymbol{\omega}_3 \cdot \mathbf{v}_3)^2}{\mu_3} \right) \right]^{\frac{1}{2}} \quad (20)$$

Table 1. Ellipsoid registration point parameters ($\Delta = d\pi/2$)

	1	2	3	4	5	6	7	8	9
u	$-\frac{\pi}{2}$	$\frac{\pi}{2} - \Delta$	$\frac{\pi}{2} + \frac{\Delta}{2}$	0	0	π	$-\frac{\pi}{2}$	$\frac{\pi}{2}$	$\frac{\pi}{2}$
v	0	0	0	$-\frac{\pi}{2} + \Delta$	$\frac{\pi}{2} - \Delta$	$\frac{\pi}{2} - \frac{\Delta}{2}$	$-\frac{\pi}{2} + \Delta$	$-\frac{\pi}{2} + \Delta$	$\frac{\pi}{2} - \Delta$

4 Methods and Results

We tested our TRE equations using computer simulations where registration transformations were computed using registration features (fiducials and model surface points) contaminated with isotropic localization noise. Our fiducial registration experiments were similar to those described in [2]. Because the square of Equation 17 is equivalent to Equation 46 from [1] we were not surprised that there was excellent agreement between the simulated RMS TRE and the predicted TRE. To conserve space for the more interesting surface registration simulations, we will omit the results from the fiducial simulations and refer the reader to [10] for results and discussion.

4.1 Surface Registration

We ran simulations of surface registration TRE using a variety of surfaces: The surfaces used were an ellipsoid, and models of two cadaver femora and the radius of a patient who underwent computer-assisted surgery. The simulations used the following steps:

1. Normally distributed noise was drawn from $\mathcal{N}(0, s_{\text{PLE}}^2/3)$ and added to the x , y , and z components of the each surface registration point.
2. The noisy point locations were registered to the surface using ICP [12]. ICP was initialized with the true registration transformation (the identity) and was run to convergence in RMS error (tolerance of 10^{-9} mm, maximum 100,000 iterations).
3. The registration was applied to the set of target locations. The displacement of a target under the registration transformation was the target registration error.

The ellipsoid had the parametric form

$$\mathbf{p}(u, v) = [150 \cos v \cos u \quad 50 \cos v \sin u \quad 25 \sin v]^T, \quad 0 \leq u \leq \pi, -\frac{\pi}{2} \leq v \leq \frac{\pi}{2}$$

and its registration points were parameterized by a scalar quantity d where $0 \leq d \leq 1$; the 9 registration points used can be computed using the values shown in Table 1. At $d = 0$ all of the points lie in the plane $x = 0$, which is the most circular cross section of the ellipsoid. The results for the ellipsoid simulations are shown in Figure 1. The predicted value of TRE agreed with the simulation results except for small values of d . The predicted TRE was large because there were small principal stiffnesses for these point configurations. The points were still close to the surface of the ellipsoid, however, so the ICP algorithm did not diverge far enough from the true registration transformation to produce the very large values of TRE predicted by the stiffness model. The predicted values of TRE as a function of target location and noise magnitude agree with the simulation results with an error of less than 2% of simulated RMS TRE.

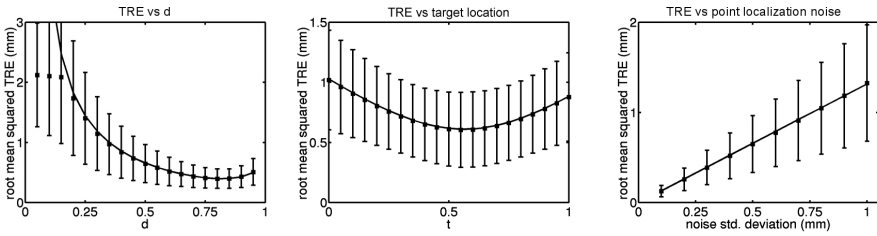


Fig. 1. Estimated (solid curve) and simulated TRE (symbols) for the ellipsoid simulations; error bars shown at ± 1 standard deviation of RMS TRE. (Left) TRE as a function of registration point location ($s_{\text{PLE}} = 0.5$ mm, target $[50\ 25\ 15]^T$). (Middle) TRE as a function of target location along the line $[-150\ -50\ -25]^T + t[300\ 100\ 50]^T$ ($s_{\text{PLE}} = 0.5$ mm, $d = 0.5$). (Right) TRE as a function of noise magnitude ($d = 0.5$, target location $[50\ 25\ 15]^T$).

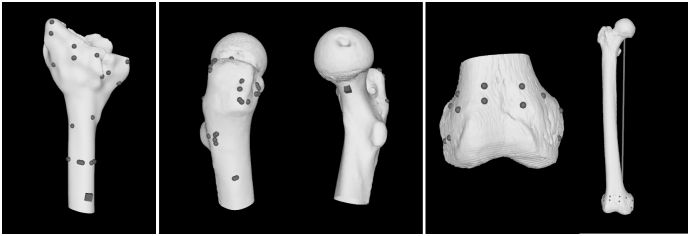


Fig. 2. Models, registration points (dark spheres), and targets (dark cubes) used for the bone surface TRE experiments. (Right) Targets are distributed along the mechanical axis of the femur for the distal femur experiment; the mechanical axis is clinically relevant in knee arthroplasty.

Target points and registration points used for the bone model experiments are shown in Figure 2. We varied the number of registration points used for the radius and proximal femur, and we varied the noise magnitude for the distal femur; results are shown in Figure 3. The predicted TRE always fell within one standard deviation of TRE magnitude for the radius and proximal femur experiments; the agreement between predicted and simulated TRE improved as the number of registration points increased. For the distal femur experiment using 14 registration points carefully selected from regions of low curvature the predicted TRE agreed with the simulated TRE with an error of less than 4% over a wide range of target locations and noise magnitude.

5 Discussion and Conclusion

We have presented analytic expressions of expected root mean square fiducial and surface target registration error. The derivation for fiducial TRE is novel and the resulting equation is equivalent to one published by [1]. Equation 20 for approximating surface TRE is unique as far as we know. The estimated surface TREs were in good agreement with our simulated values.

The reliability of Equation 20 can be compromised in realistic situations because of the strong dependence on the normal vectors \mathbf{n}_i . We would caution against relying on

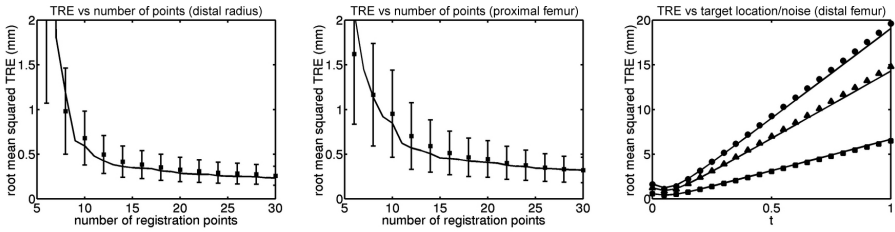


Fig. 3. Estimated (solid curve) and simulated TRE (symbols) for the bone surface simulations; error bars shown at ± 1 standard deviation of RMS TRE. (Left) TRE as a function of the number of registration points for the distal radius. (Middle) TRE as a function of the number of registration points for the proximal femur. (Right) TRE as a function of target location along the line of the mechanical axis (parameterized by t) and noise magnitude for the distal femur experiment ($s_{\text{PLE}} = 0.35, 0.75, 1.0$ mm).

Equation 20 if points are selected from surfaces with high curvature features. Nevertheless, we believe that Equation 20 is a useful tool for studying surface-based registration and we have already applied it the optimization of registration point selection [10].

References

1. Fitzpatrick, J.M., et al.: Predicting error in rigid-body point-based registration. *IEEE Trans Med Imaging* **17**(5) (1998) 694–702
2. Maurer Jr., C.R., et al.: Registration of head volume images using implantable fiducial markers. *IEEE Trans Med Imaging* **16**(4) (1997) 447–462
3. Evans, A.C., et al.: Image registration based on discrete anatomic structures. In Maciunas, R.J., ed.: *Interactive Image-Guided Neurosurgery*. American Association of Neurological Surgeons, Park Ridge, IL (1993) 63–80
4. Hill, D.L.G., et al.: Accurate frameless registration of MR and CT images of a head: Applications in surgery and radiotherapy planning. *Radiology* **191** (1994) 447–454
5. Ellis, R.E., et al.: A method for evaluating CT-based surgical registration. In Troccaz, J., Grimson, E., Mösges, R., eds.: *CVRMed-MRCAS'97*. LNCS 1205, Grenoble, France, Springer (1997) 141–150
6. Ma, B., Ellis, R.E.: Spatial-stiffness analysis of surface-based registration. In Barillot, C., Haynor, D., Hellier, P., eds.: *MICCAI2004*. LNCS 3216, Springer (2004) 623–630
7. Lin, Q., et al.: A stiffness-based quality measure for compliant grasps and fixtures. *IEEE Trans Robot Automat* **16**(6) (2000) 675–688
8. Ma, B., Ellis, R.E.: A spatial-stiffness analysis of fiducial registration accuracy. In Ellis, R.E., Peters, T.M., eds.: *MICCAI2003*. Volume 1 of LNCS 2879., Springer (2003) 359–366
9. Meriam, J.L., Kraige, L.G.: *Engineering Mechanics: Dynamics*. John Wiley and Sons (1986)
10. Ma, B.: *A Unified Approach to Surface-Based Registration for Image-Guided Surgery*. PhD thesis, Queen's University, Kingston, Ontario, Canada (2005)
11. Ross, S.M.: *Introduction to Probability Models*. 7th edn. Academic Press (2000)
12. Besl, P., McKay, N.: A method for registration of 3-D shapes. *IEEE Trans Pattern Anal* **14**(2) (1992) 239–256